FEBS Letters 508 (2001) 282–286 FEBS 25469

Gelsolin overexpression enhances neurite outgrowth in PC12 cells

Elizabeth J. Furnish[a], Wei Zhou[c], Casey C. Cunningham[d], Josef A. Kas[b,c], Christine E. Schmidt[a,c,*]

[a] *Department of Chemical Engineering, 26th and Speedway, MC C0400, University of Texas at Austin, Austin, TX 78712, USA*
[b] *Department of Physics, University of Texas at Austin, Austin, TX 78712, USA*
[c] *Institute for Cellular and Molecular Biology, University of Texas at Austin, Austin, TX 78712, USA*
[d] *Physicians Reliance Network, Inc., 3535 Worth Street, Dallas, TX 75246, USA*

Received 7 August 2001; revised 23 October 2001; accepted 23 October 2001

First published online 2 November 2001

Edited by Amy McGough

Abstract The rational design of therapies for treating nerve injuries requires an understanding of the mechanisms underlying neurite extension. Neurite motility is driven by actin polymerization; however, the mechanisms are not clearly understood. One actin accessory protein, gelsolin, is involved with remodeling the cytoskeleton, although its role in cell motility is unclear. We report a two-fold upregulation of gelsolin upon differentiation with nerve growth factor. Cells that were genetically modified to overexpress gelsolin have longer neurites and a greater neurite motility rate compared to controls. These data suggest that gelsolin plays an important role in neurite outgrowth. © 2001 Published by Elsevier Science B.V. on behalf of the Federation of European Biochemical Societies.

Key words: Actin cytoskeleton; Gelsolin; Neurite outgrowth; PC12 cell; Growth cone motility

1. Introduction

Neurite (e.g. axon) extension involves assembly and disassembly of actin filaments in growth cones, which are specialized structures at neurite tips that guide axonal extension [1]. Several studies have demonstrated addition of actin monomers at the leading edges of growth cones and successive rearward translocation of actin filaments [2–4]. Similar actin dynamics are observed in motile cells such as fibroblasts [5]. Neurite elongation and cell locomotion are both driven by indirect connections made between these rearward-moving actin filaments and the substrate [1,4,6].

A number of actin accessory proteins, such as gelsolin, regulate actin dynamics. Calcium activates gelsolin to disassemble actin filaments by severing and capping them at their plus ends, where polymerization occurs [7]. However, phosphoinositides bind to gelsolin and cause it to release the actin filament, thereby allowing repolymerization to take place [8,9]. The overall effect of the cycle of gelsolin activation and inactivation is a net increase in the number of actin filament plus ends as sites for actin polymerization.

Previous experiments indicate that the importance of gelsolin for actin-based motility is uncertain. For example, fibroblasts with increased gelsolin levels migrated faster than controls [10], but neurons from gelsolin null mice extended neurites at the same rate as controls [11]. Overexpression of truncated gelsolin in neurons led to decreased neurite length and loss of actin filaments [12]. Because this truncation removes the calcium requirement for gelsolin activation, this negative effect on neurite outgrowth suggests that, without regulation, gelsolin can have a detrimental effect on actin-based motility. In addition, cells microinjected with gelsolin showed a destructive loss of actin filaments with only certain preparations of gelsolin [13,14]. Therefore, it is not clear whether gelsolin is critical for actin-based cell migration events, particularly for neurite extension.

Our experiments seek to clarify the relationship between gelsolin and neurite outgrowth. We have used the PC12 (pheochromocytoma) neuronal-like cell line that extends neurites when differentiated with nerve growth factor (NGF) [15]. We report for the first time an upregulation of gelsolin in PC12s coinciding with NGF-induced neurite outgrowth. This upregulation suggests that gelsolin plays a key role in neurite extension. To determine whether gelsolin overexpression enhances neurite outgrowth, human gelsolin cDNA was transfected into PC12s. We found a dramatic increase in neurite length and motility rate for cells overexpressing gelsolin compared to controls. Thus, our results suggest that an increased level of gelsolin enhances neurite outgrowth and motility, most likely via an increase in actin filament turnover.

2. Materials and methods

2.1. Cell culture

Chemicals and materials were purchased from Sigma (St. Louis, MO, USA) unless noted. PC12 cells, a rat pheochromocytoma cell line that responds to NGF by expressing 'neurite-like' processes, were purchased from the American Type Culture Collection (Manassas, VA, USA). PC12 cells were cultured in 85% RPMI supplemented with 10 mM 4-(2-hydroxyethyl)piperazine-1-ethanesulfonic acid, 25 mM glucose, 1 mM sodium pyruvate, 10% horse serum (JRH Biosciences, Lenexa, KS, USA), and 5% fetal bovine serum. Cells were maintained at 37°C in a humidified 5% CO_2 incubator. Medium was replaced every 2–3 days, and cells were passaged with 1 mM ethylenediaminetetraacetic acid or by trituration. For neurite outgrowth experiments, 50 ng/ml 2.5S NGF (Invitrogen, Carlsbad, CA, USA) was added to the culture medium.

2.2. Transfection

Stable gelsolin clones were created by transfecting PC12s using Lipofectin (Invitrogen) with the LKCG plasmid, which contains the cDNA for human cytoplasmic gelsolin in the LK444 expression vector [16]. Mock-transfected clones were created using the LK444 plasmid.

*Corresponding author. Fax: (1)-512-471 7060.
E-mail address: schmidt@che.utexas.edu (C.E. Schmidt).

Abbreviations: NGF, nerve growth factor; PC12, pheochromocytoma

0014-5793/01/$20.00 © 2001 Published by Elsevier Science B.V. on behalf of the Federation of European Biochemical Societies.
PII: S0014-5793(01)03078-2

Lipofectin was used according to the manufacturer's instructions and as described specifically for PC12s [17]. Briefly, cells were seeded at $1–1.5\times10^4$ cells/cm^2 and cultured for 24 h before transfection. Cells were cultured with 15 μg/ml Lipofectin and 10 μg/ml DNA for 3–5 h. After 3 days, cells were cultured under selection pressure (0.3 mg/ml G418).

2.3. Cell lysis

Cells were lysed on ice for 30 min in Triton extraction buffer supplemented with a protease inhibitor cocktail (Sigma P8340, 100 μl/ml) as described [10]. Lysates were vortexed with glass beads (425–600 μm), then centrifuged at $10\,000\times g$ for 10 min. The glass beads are used to help disrupt the cell membrane, break up protein complexes and shear DNA [18]. When the lysis mixtures are centrifuged, the glass beads pellet with the membrane fraction. Control studies show that gelsolin does not bind to the glass beads and remains in the soluble fraction. The total protein concentration of each lysate was determined using a Bradford-based protein assay (Bio-Rad, Hercules, CA, USA) and a spectrophotometric plate reader (ELX800; SciMetrics, Missouri City, TX, USA). Electrophoresis sample buffer was added to lysates before boiling for 3 min.

2.4. Immunoblot analysis

Lysates were electrophoresed on 7.5% polyacrylamide gels and transferred to polyvinylidene difluoride membranes (Bio-Rad). Bovine plasma gelsolin standards were included in each immunoblot. After blocking with 5% bovine serum albumin (Jackson ImmunoResearch, West Grove, PA, USA) for 1–4 h at room temperature, membranes were probed with a goat anti-gelsolin polyclonal antibody (1:200; Santa Cruz Biotechnology, Santa Cruz, CA, USA) overnight at 4°C and a horseradish peroxidase-conjugated anti-goat secondary antibody (1:25 000; Santa Cruz Biotechnology) for 1 h at room temperature. An enhanced chemiluminescent substrate (Pierce Chemical, Rockford, IL, USA) was used to detect bands. Blots were quantified by densitometry using NIH Image software. Only bands within the linear range of optical density as determined by gelsolin standards were analyzed. Two to five samples were run for each independent experiment, and the results from two to four independent experiments were averaged for quantitation. The total number of samples from all experiments is reported in the text.

2.5. RNA isolation and RT-PCR

Total RNA was isolated from each clone using the RNAqueous™-4PCR kit (Ambion, Austin, TX, USA). RNA concentration was determined using spectrophotometry, and 5 μg of total RNA from each sample was used in the reverse transcriptase reactions (RETROscript™ kit, Ambion). The gelsolin gene was then amplified by PCR to generate a 289 bp fragment using the following primers: 5′-ACTGGTCTACTGTGTCTCTA-3′ and 5′-TCTTCAGCCCACACTTTCTG-3′ [19]. 18S RNA was amplified in parallel to generate a 489 bp fragment as a loading control (QuantumRNA™ Classic 18S Internal Standards, Ambion). For visualization, 1 μCi [α-^{32}P]dATP was added to the reaction, which was performed in a Perkin-Elmer 2400 thermal cycler using 25 cycles: denaturing at 94°C for 30 s, annealing at 60°C for 30 s, and extension at 72°C for 2 min, with a final extension at 72°C for 5 min. PCR products were run on 6% polyacrylamide gels. Radioactive bands were detected using a phosphorimager (445SI, Molecular Dynamics, Sunnyvale, CA, USA).

2.6. Neurite length measurement and neurite extension rate analysis

Cells were seeded at 10^4 cells/cm^2 on tissue culture polystyrene and cultured for up to 10 days with NGF. Phase contrast images were acquired using either a 10 or 20× objective on an Olympus IX70 (Melville, NY, USA) microscope. Neurite length was quantified using a modified neurite length macro (ftp://rsbweb.nih.gov/pub/nih-image/user-macros). Neurites less than 10 μm in length or whose starting and ending points were not clearly evident were excluded from the computation of the median neurite length. PC12 cells grow short spontaneous protrusions in the absence of NGF, and it is common to exclude these short neurites to ensure they are not included in the analysis of true neurite extension. In addition, these short protrusions (< 10 μm) are difficult to accurately measure in terms of length. Median neurite lengths for each image were averaged to determine the overall average neurite length. The reported value for n is the total number neurites measured. Neurites were measured for a minimum of two to 10 images. Average neurite extension rates were computed from neurite outgrowth data as the net positive distance (defined as net extension away from the cell body) traveled per total elapsed time. In other words, the average neurite length was divided by the total observation time to obtain the average extension rate.

2.7. Video microscopic analysis of neurite motility

Cells were cultured as described for neurite length experiments for up to 3 days with NGF. During image acquisition, conditions of pH 7.2 and 37°C were maintained. Digital images were recorded every 2 min for up to 7 h using a computer-controlled stage (Ludl Electronics, Hawthorne, NY, USA) and a 24-bit color CCD video camera (Hamamatsu). In each image, a stationary feature was used as a reference point to account for slight variations of the computer-controlled stage. To calculate neurite motility rate (μm/h), the absolute distance traveled by each neurite tip over 10 min intervals (regardless of direction) was divided by the time. The net extension was not tracked in these studies. These motility rates thus represent the 'motile activity' of neurite extension and retraction. The reported value for n is the number of neurites monitored for motility.

2.8. Statistical analysis

Student's t-test was used to determine statistical significance of differences between gelsolin expression level, neurite length, extension rate for gelsolin clones compared to those of controls. A significance level of $P < 0.05$ (> 95% confidence level) was used. Averages are reported ± S.E.M.

3. Results and discussion

3.1. Gelsolin upregulation in PC12 cells upon differentiation with NGF

PC12 cells extend neurites by an actin-based process in the presence of NGF. During differentiation with NGF in the present studies, a two-fold upregulation of gelsolin from 0.91 ± 0.07 ($n=4$) to 2.07 ± 0.18 ($n=4$) mg gelsolin/g protein ($P<0.05$, Fig. 1) was measured, which is qualitatively illustrated by the immunoblot (Fig. 1, inset). Upregulation of gelsolin in the cells was measured after 5 days in NGF. Previous reports qualitatively examined gelsolin expression in PC12s, but an upregulation was not seen for shorter exposures to NGF [20]. In other cell types, gelsolin upregulation during differentiation, which coincides with actin remodeling, has been reported [21–23]. The increase shown here suggests that gelsolin is important for neurite extension because its upregulation is correlated with neurite outgrowth.

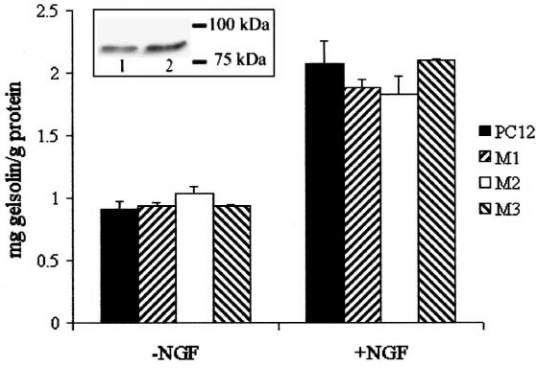

Fig. 1. Gelsolin is upregulated in PC12 cells and mock clones upon differentiation with NGF. Quantified gelsolin expression levels from immunoblot analysis show gelsolin expression levels, after 5 days exposure to NGF, that are normalized to the grams of whole cell lysate protein. Results represent the average ± S.E.M. ($n=4$). The inset shows an immunoblot of whole cell lysates (20 μg/lane) from PC12s that were cultured in the absence (lane 1) or presence (lane 2) of NGF. The molecular weight markers on the right indicate that gelsolin is ~90 kDa.

3.2. Initial characterization of transfected clones

To test our hypothesis that increased gelsolin expression enhances neurite outgrowth, we created gelsolin-transfected (G) clones and mock-transfected (M) clones. First, to characterize the control cells, mock clones M1–M3 were assayed for gelsolin expression levels and neurite outgrowth. Like PC12s, all mock clones show a two-fold upregulation of gelsolin when exposed to NGF (Fig. 1). In addition, the mock clones exhibit neurite lengths (ranging from 13.8 ± 2.1 to 16.8 ± 1.1 μm, $n = 20$–606) comparable to those of PC12s (15.5 ± 0.6 μm, $n = 151$) when exposed to NGF for 2 days. Therefore, the data suggest that there is little to no significant clonal variation in gelsolin expression and neurite outgrowth for PC12s. Mock clone M2 was selected as the control for all studies.

Gelsolin expression levels for nine gelsolin clones were also evaluated. The gelsolin expression level in the absence of NGF for gelsolin clone G3 (1.86 ± 0.12 mg gelsolin/g protein, $n = 8$) is significantly greater than that for the mock clone M2 (1.04 ± 0.05 mg gelsolin/g protein, $n = 8$, $P < 0.01$; Fig. 2 and inset A). This overexpression is also shown for mRNA levels (Fig. 2, inset B). Only clone G3 efficiently expressed the transfected gene and was selected for further study.

3.3. Gelsolin expression characteristics for clones M2 and G3

The effect of NGF differentiation on gelsolin expression was examined in more detail for clones M2 and G3 (Fig. 2). Within 3 days of exposure to NGF, clone M2 shows an approximate two-fold increase in gelsolin expression levels ($P < 0.01$). After 3 days, the gelsolin level reaches a plateau, suggesting the existence of an optimal level of gelsolin expression for neurite outgrowth. In contrast, the gelsolin level in the absence of NGF for gelsolin clone G3 is initially elevated compared to that for mock clone M2, but is not further upregulated upon differentiation with NGF. This lack of upregulation further supports the concept of an optimal gelsolin level for neurite extension.

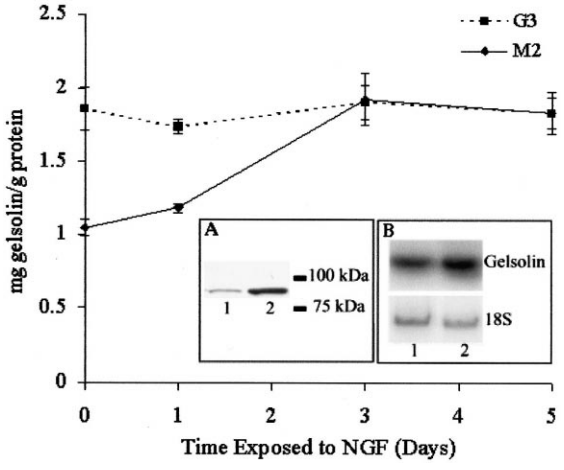

Fig. 2. Gelsolin is overexpressed in clone G3. Quantified data of gelsolin expression for mock clone M2 and gelsolin clone G3 upon exposure to NGF for up to 5 days. Results represent the average ± S.E.M. ($n = 8$). Solid line, M2; dashed line, G3. Inset A: Immunoblot (20 μg/lane) indicating that gelsolin expression in the absence of NGF for gelsolin clone G3 (lane 2) is greater than that for mock clone M2 (lane 1). Inset B: The gelsolin mRNA level in the absence of NGF for gelsolin clone G3 (lane 2) is greater than that for mock clone M2 (lane 1). Levels of 18S mRNA are similar.

3.4. Gelsolin overexpression enhances neurite length and neurite extension rate

To determine the effect of gelsolin overexpression on neurite outgrowth, clones G3 and M2 were cultured in NGF for up to 10 days. Phase contrast images illustrate the enhancement of neurite length for clone G3 compared with that for mock clone M2 in the absence and presence of NGF for 2 days (Fig. 3A).

In the absence of NGF, the average neurite length for clone G3 (19.3 ± 2.5 μm, $n = 14$) is greater than that of mock clone M2 (13.0 ± 1.5 μm, $n = 6$, $P < 0.01$, Fig. 4A). For assessment of neurite length, only neurites > 10 μm were measured (as described in Section 2). The numbers of neurites meeting these conditions are small for both clones, since PC12s require stimulation with NGF to undergo differentiation. However, the total number of neurites exceeding 10 μm is greater for the G3 clone compared to that for the M2 clone. Therefore, these data suggest that an increased gelsolin level gives PC12s a 'head start' for neurite outgrowth. Furthermore, the average density of all spontaneous neurites (number of neurites/cell) is 1.7 ± 0.31 ($n = 62$) for G3 cells and 0.7 ± 0.2 for M2 cells ($n = 156$), which represents over a two-fold increase in the number of spontaneous neurites for the G3 clone compared to that for the M2 clone ($P \ll 0.001$). These data further support the hypothesis that increased levels of gelsolin give G3 cells a head start and thus prepare the cells for neurite outgrowth by increasing the density of short, spontaneous neurites.

After 2 days in the presence of NGF, the average neurite length for clone G3 is increased 100% compared to that for mock clone M2 ($P \ll 0.001$) (Figs. 3C and 4A). The histograms in Fig. 3C clearly illustrate an increase in the number of neurites with longer lengths for the G3 cells after 2 days exposure to NGF (i.e. the distribution in the histogram for G3 is shifted to the right compared to that for M2). The average neurite length for gelsolin clone G3 decreases slightly after 4 days exposure to NGF (Fig. 4A); however, this trend most likely reflects the exclusion of longer neurites from analysis. As neurites grow in the presence of NGF, they become more 'networked', and their starting and ending points are not clearly distinguishable (Fig. 3A,B). Therefore, some longer neurites are excluded from the analysis, which leads to a slight underestimation of neurite length.

For mock clone M2, the average neurite length increases from 16.7 ± 0.6 μm ($n = 606$) at day 2 to 20.3 ± 0.6 μm ($n = 799$) at day 4 (Fig. 4A). The neurite length for M2 after 8 and 10 days in the presence of NGF (23.4 ± 2.3, $n = 45$ and 31.2 ± 3.8 μm, $n = 75$, respectively) begins to approach that for the gelsolin clone G3 at 2 days. Thus, mock clone M2 appears to go through a lag period of several days before increasing neurite outgrowth to the level attained for G3 at earlier times.

The corresponding average neurite extension rates (Fig. 4B), calculated as net neurite extension for a total elapsed time, illustrate that neurite extension rate is elevated for G3 at all times, and is most enhanced for G3 compared to M2 at early time points. This further suggests that an enhanced gelsolin level may give PC12s a 'head start' for neurite outgrowth. Again, the exclusion of longer, networked neurites at longer times may skew these results slightly.

Our results suggest that gelsolin plays an important role in neurite outgrowth. On the other hand, as mentioned earlier, studies using gelsolin null mice illustrate that there is no sig-

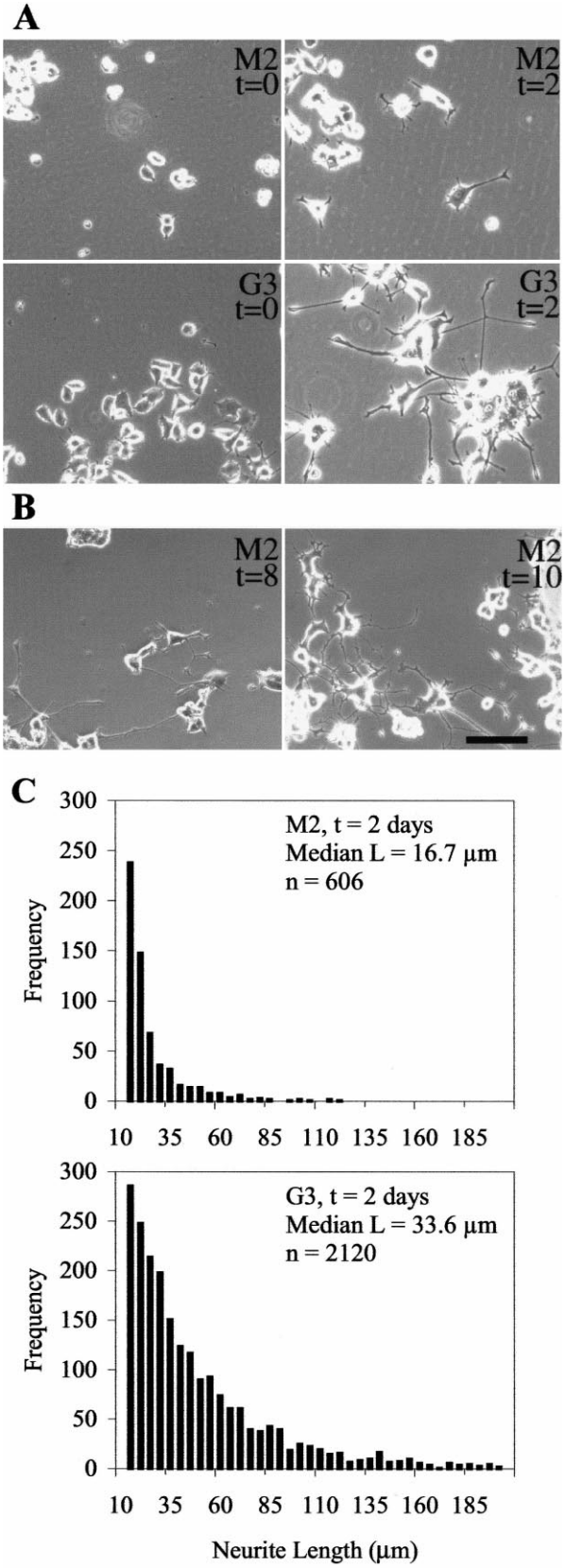

Fig. 3. Neurite lengths are increased for clone G3. A: Phase contrast images are shown for clones M2 and G3 cultured in the absence ($t=0$) and presence of NGF for 2 days ($t=2$). B: Phase contrast images are shown for clone M2 cultured in the presence of NGF for 8 and 10 days ($t=8$, $t=10$). Bar, 100 µm. C: Histograms show the distribution of neurite lengths (frequency of neurites having a given length versus the length) for clones M2 and G3 after $t=2$ days.

nificant difference in neurite extension for neurons lacking gelsolin compared to controls. In the gelsolin null mice, there are likely redundant actin accessory proteins that compensate for the activity when gelsolin is completely removed. These knock-out experiments are designed to provide insight into the role of essential and non-essential proteins. If an important, but non-essential, protein is targeted, then one may still see function as a result of redundant mechanisms. These results indicate that gelsolin is not essential, but that it may still be important, as suggested by our studies.

3.5. Gelsolin overexpression enhances neurite motility

Because neurite extension is a dynamic process, we determined whether gelsolin overexpression enhances neurite motility in addition to increasing net neurite length. To compute inherent neurite motility, the absolute distance (regardless of direction) traveled per time was assessed for each neurite using video microscopy. The net extension was not tracked in these studies. These motility rates thus represent the 'motile activity' of neurite extension and retraction.

Plots of neurite motility for M2 and G3 after 2 days exposure to NGF are shown in Fig. 5A. The increase in the amplitude of the motility peaks for clone G3 compared to that for mock clone M2 indicates that gelsolin overexpression

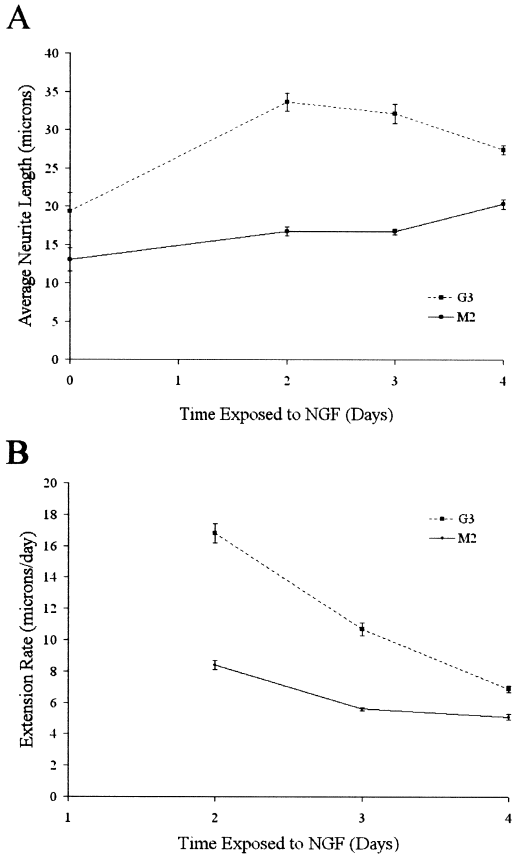

Fig. 4. Neurite lengths and neurite extension rate are enhanced for clone G3. A: Average neurite lengths for clones M2 and G3 for up to 4 days. Results represent the average ± S.E.M. G3, day 0: $n=14$; G3, day 2: $n=2120$; G3, day 3: $n=975$; G3, day 4: $n=1482$; M2, day 0: $n=6$; M2, day 2: $n=606$; M2, day 3: $n=402$; M2, day 4: $n=799$. Note: The error bars for G3 at time 0 are too small to be seen on the plot. B: Neurite extension rates for G3 and M2 cells after 2, 3 and 4 days. The extension rate was computed as the net extension of the neurite after total elapsed time in NGF. Solid line, M2; dashed line, G3.

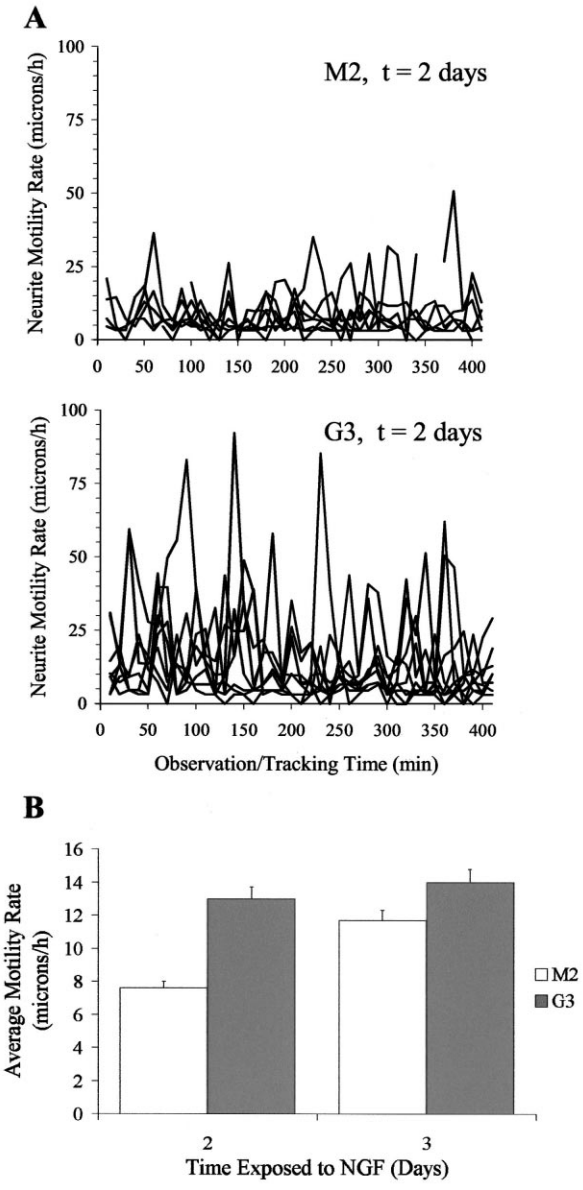

Fig. 5. Neurite motility rate (i.e. activity) is enhanced for clone G3. A: Neurite motility rate over observation time for M2 and G3 clones after 2 days exposure to NGF. Each line represents the fluctuating motility of a single neurite as it is tracked over time. The height (amplitude) and number of peaks indicate the 'activity' of the cells. The individual paths are not represented so that they can be distinguished. These plots are intended to provide an overall visual representation of the motility or activity of the neurites for G3 compared to M2. Discontinuities in some of the lines reflect neurites that initiated extension or retraction or became obstructed from view after the onset of image acquisition. B: Average neurite motility rates (computed from the individual paths presented in A) after 2 and 3 days exposure to NGF are shown for clones M2 and G3. Results represent the average ± S.E.M.

enhances neurite motility (i.e. activity). After 2 days in the presence of NGF, the average motility rate for gelsolin clone G3 ($n = 9$) is greater compared to that for mock clone M2 ($n = 8$, $P < 0.001$), but remains relatively constant after 3 days ($n = 10$) (Fig. 5B). In contrast, the motility rate after 3 days for clone M2 ($n = 8$) increases to approach the level seen for G3, suggesting that clone M2 lags behind clone G3 in neurite motility.

4. Summary

Our results demonstrate that gelsolin expression is upregulated upon differentiation of PC12s with NGF. Furthermore, when gelsolin is elevated at early time points, neurite length and motility are increased. Because gelsolin affects actin dynamics by severing, capping, and releasing actin filaments to create more nucleation sites, the enhancing effect of gelsolin on neurite length and motility is most likely a result of an increase in actin filament turnover and repolymerization, which then drives neurite extension. Although the exact mechanism behind the enhanced neurite elongation for our system is not known, such information is important for understanding the processes that control neurite extension and may ultimately help to design treatments for nerve injuries.

Acknowledgements: The authors wish to thank Dr. Peter Vize for assistance with RT-PCR experiments, Dr. Charles Patrick, Jr. and Eric Brey for the use of and assistance with their video microscopy facilities, and Matthew Schmid, Hyma Durgam, Suzanne Bowers, Gabriella Ramos, and Mario Luis Ramirez for their help with experiments and data analysis. This work was supported by a Whitaker Foundation Grant (C.E.S.), National Science Foundation Graduate Research Fellowship (E.J.F.) and Grants (BES-9733156, C.E.S.; MCB-9808849, J.A.K.), National Institutes of Health Grant (1R29AR45008-01, J.A.K.), and a gift from the Longenbaugh Foundation (C.E.S.).

References

[1] Lin, C.H., Thompson, C.A. and Forscher, P. (1994) Curr. Opin. Neurobiol. 4, 640–647.
[2] Okabe, S. and Hirokawa, N. (1991) J. Neurosci. 11, 1918–1929.
[3] Forscher, P. and Smith, S.J. (1988) J. Cell Biol. 107, 1505–1516.
[4] Mitchison, T. and Kirschner, M. (1988) Neuron 1, 761–772.
[5] Lauffenburger, D.A. and Horwitz, A.F. (1996) Cell 84, 359–369.
[6] Suter, D.M. and Forscher, P. (2000) J. Neurobiol. 44, 97–113.
[7] Yin, H.L., Hartwig, J.H., Maruyama, K. and Stossel, T.P. (1981) J. Biol. Chem. 256, 9693–9697.
[8] Janmey, P.A. and Stossel, T.P. (1987) Nature 325, 362–364.
[9] Lin, K.M., Wenegieme, E., Lu, P.J., Chen, C.S. and Yin, H.L. (1997) J. Biol. Chem. 272, 20443–20450.
[10] Cunningham, C.C., Stossel, T.P. and Kwiatkowski, D.J. (1991) Science 251, 1233–1236.
[11] Lu, M., Witke, W., Kwiatkowski, D.J. and Kosik, K.S. (1997) J. Cell Biol. 138, 1279–1287.
[12] Westberg, J.A., Zhang, K.Z. and Andersson, L.C. (1999) FASEB J. 13, 1621–1626.
[13] Huckriede, A., Fuchtbauer, A., Hinssen, H., Chaponnier, C., Weeds, A. and Jockusch, B.M. (1990) Cell Motil. Cytoskel. 16, 229–238.
[14] Cooper, J.A., Bryan, J., Schwab, B., Frieden, C., Loftus, D.J. and Elson, E.L. (1987) J. Cell Biol. 104, 491–501.
[15] Greene, L.A. and Tischler, A.S. (1976) Proc. Natl. Acad. Sci. USA 73, 2424–2428.
[16] Gunning, P., Leavitt, J., Muscat, G., Ng, S.Y. and Kedes, L. (1987) Proc. Natl. Acad. Sci. USA 84, 4831–4835.
[17] Muller, S.R., Sullivan, P.D., Clegg, D.O. and Feinstein, S.C. (1990) DNA Cell Biol. 9, 221–229.
[18] Moncman, C. (2001) Personal communication, University of Kentucky Medical Center.
[19] Huang, L. and Pardee, A.B. (2000) Mol. Med. 6, 849–866.
[20] Tanaka, J., Kira, M. and Sobue, K. (1993) Dev. Brain Res. 76, 268–271.
[21] Olsen, E., Rasmussen, H.H. and Celis, J.E. (1995) Electrophoresis 16, 2241–2248.
[22] Onoda, K., Yu, F.X. and Yin, H.L. (1993) Cell Motil. Cytoskel. 26, 227–238.
[23] Dieffenbach, C.W., SenGupta, D.N., Krause, D., Sawzak, D. and Silverman, R.H. (1989) J. Biol. Chem. 264, 13281–13288.